

Molecular and electronic structures of six-coordinate chloro-oxo-metalate complexes of V, Nb, Ta, Mo, and W

Adam J. Bridgeman^{*a} and Germán Cavigliasso^{a,b}

^a Department of Chemistry, University of Hull, Kingston upon Hull, UK HU6 7RX.

E-mail: A.J.Bridgeman@chem.hull.ac.uk

^b Department of Chemistry, University of Cambridge, Lensfield Road, Cambridge, UK CB2 1EW

Received 19th March 2001, Accepted 22nd October 2001

First published as an Advance Article on the web 27th November 2001

The molecular and electronic structures of anionic $[\text{MO}_n\text{Cl}_{6-n}]^-$ ($n = 1-3$) complexes of V, Nb, Ta, Mo and W have been investigated using density-functional methods. Calculated structural parameters, including geometries and vibrational frequencies, are in good agreement with reported experimental data. A detailed bonding analysis is presented, and the properties of relevance to modelling polyoxoanion chemistry are explored and discussed. Structural *trans*-influence phenomena have been observed in all species studied. A combined analysis based on Mulliken–Mayer population methods and geometrical and bonding-energy data, supports the idea that both electronic and electrostatic factors are involved in the *trans* influence. Valuable insight into the redox properties of mono-oxo and *cis* di-oxo complexes, and the connection with polyoxometalates, has been gained by probing the nature of frontier orbitals. In general, bonding interactions possess metal-d and ligand-p character, and are strongly covalent in M–O bonds, and from moderately to largely ionic in M–Cl bonds.

Introduction

Vanadium, molybdenum, tungsten, and to a lesser extent niobium and tantalum stand out amongst the transition metals in their ability to form polymeric oxoanions. These polyoxoanions or polyoxometalates constitute an immense class of compounds in number and diversity,^{1,2} and exhibit remarkable chemical and physical properties, their actual and potential applications spanning a variety of fields, including medicine, catalysis, solid-state technology, and chemical analysis.²⁻⁴

The structures of polyoxometalates can be characterized as an assemblage of MO_n coordination polyhedra, the octahedron being the most commonly observed constituent unit.¹ A classification scheme based on the number of terminal M–O bonds at the metal centres has been proposed by Pope,^{1,2} and has proven useful and convenient for the rationalization of electron-transfer properties. The vast majority of polyoxoanion structures (based on MO_6 units) contain no more than two unshared O atoms in each polyhedral unit, and are thus classified as type-I if there is one terminal M–O bond, or as type-II, if two such bonds are present in a *cis* spatial arrangement. Some authors⁵ have also included a type-III category, which describes structures that incorporate both type-I and type-II octahedra.

The redox behaviour of polyoxometalates is directly related to the number of terminal M–O bonds at the metal centres. Thus, type-I structures undergo reversible reductions, which yield mixed-valence species (called “heteropoly blues”), with minor structural changes, whereas type-II systems are reduced irreversibly, and with more difficulty.^{1,2} These different redox properties of polyanions have been rationalized in terms of the electronic structures of $[\text{MO}_5]$ and *cis*- $[\text{MO}_2\text{L}_4]$ complexes, which represent model systems for type-I and type-II octahedral units, respectively.^{1,6} The most important factor is the nature of the lowest-unoccupied molecular orbital (LUMO)—the orbital occupied by the additional electrons in the reduced species—which is (in principle) nonbonding in the $[\text{MO}_5]$ system, but M–O antibonding in the *cis*- $[\text{MO}_2\text{L}_4]$ system. A correlation therefore appears to exist between the bonding

characteristics of the model monomers and the electron-transfer behaviour observed in the polymeric structures.

Metal–ligand multiple bonds constitute an active field in transition-metal computational research.⁷⁻¹³ In particular, considerable attention has been focused on complexes of the oxo type,^{9,11,13} in part due to the biological importance of some of these species. However, systematic investigations of the structural and electronic properties of simple oxo complexes that are directly connected to polyoxoanion chemistry have, to the best of our knowledge, not been conducted.

In this article we report the results of density-functional calculations on a series of chloro-oxo-metalate complexes which serve as models for type-I ($[\text{MOCl}_5]^{n-}$) and type-II (*cis*- $[\text{MO}_2\text{Cl}_4]^{n-}$) systems, and also for the rather special case of polyoxometalates containing three terminal M–O bonds (*fac*- $[\text{MO}_3\text{Cl}_3]^{n-}$). We have carried out an extensive structural characterization by means of geometry optimizations and vibrational analysis of (formally) d^0 , d^1 , and d^2 species, and we have explored, using molecular-orbital theory, population methods, and bonding-energy analyses, those aspects of the electronic structure of these complexes that are most relevant to the bonding and redox properties of the polymeric anions. Research on the structure and bonding in $[\text{MO}_4]^{n-}$ and $[\text{M}_2\text{O}_7]^{n-}$ oxoanions of V, Nb, Ta, Mo, and W has already been completed,^{14,15} and work on several more complex polyoxometalates is in progress.

Computational approach

All density-functional calculations reported in this work were performed with the ADF^{16,17} program. Functionals based on the Vosko–Wilk–Nusair¹⁸ (VWN) form of the Local Density Approximation¹⁹ (LDA), and on a combination (labelled BP86) of Becke’s 1988 exchange²⁰ and Perdew’s 1986 correlation²¹ corrections to the LDA were employed. Slater-type-orbital (STO) basis sets of triple-zeta quality incorporating frozen cores and the ZORA relativistic approach (ADF type-IV)^{16,17} were utilized.

Table 1 Optimized geometries for $[\text{MOCls}]^n$ complexes (M–O and M–Cl distances in pm, O–M–Cl angles in degrees). Available experimental results are given in parentheses

| Molecule | M–O | M–Cl _e | M–Cl _a | O–M–Cl _e |
|-------------------------|-----------|-------------------|-------------------|---------------------|
| $[\text{VOCl}_3]^{2-}$ | 159 | 234 | 246 | 93 |
| $[\text{NbOCl}_3]^{2-}$ | 174 (181) | 245 (241) | 260 (257) | 94 (96) |
| $[\text{TaOCl}_3]^{2-}$ | 177 | 244 | 262 | 94 |
| $[\text{MoOCl}_3]^-$ | 171 | 235 | 244 | 94 |
| $[\text{MoOCl}_3]^{2-}$ | 170 | 242 | 252 | 94 |
| $[\text{MoOCl}_3]^{3-}$ | 170 | 255 | 264 | 94 |
| $[\text{WOCl}_3]^-$ | 173 (167) | 235 (237) | 245 (267) | 94 (97) |
| $[\text{WOCl}_3]^{2-}$ | 173 (172) | 242 (240) | 254 (256) | 94 (94) |
| $[\text{WOCl}_3]^{3-}$ | 173 | 252 | 268 | 94 |

Table 2 Optimized geometries for $[\text{MO}_2\text{Cl}_4]^n$ and $[\text{MO}_3\text{Cl}_3]^{3-}$ complexes of Mo and W (M–O and M–Cl distances in pm, O–M–O, Cl_e–M–Cl_e, and *trans* O–M–Cl angles in degrees)

| Parameter | $[\text{MoO}_2\text{Cl}_4]^{2-}$ | $[\text{MoO}_2\text{Cl}_4]^{3-}$ |
|------------------------------------|----------------------------------|----------------------------------|
| M–O | 173 | 175 |
| M–Cl _e | 244 | 257 |
| M–Cl _t | 255 | 276 |
| O–M–O | 103 | 111 |
| Cl _e –M–Cl _e | 170 | 179 |
| Cl _t –M–Cl _t | 82 | 79 |
| Parameter | $[\text{WO}_2\text{Cl}_4]^{2-}$ | $[\text{WO}_2\text{Cl}_4]^{3-}$ |
| M–O | 175 | 177 |
| M–Cl _e | 243 | 254 |
| M–Cl _t | 256 | 276 |
| O–M–O | 102 | 110 |
| Cl _e –M–Cl _e | 169 | 180 |
| Cl _t –M–Cl _t | 81 | 79 |
| Parameter | $[\text{MoO}_3\text{Cl}_3]^{3-}$ | $[\text{WO}_3\text{Cl}_3]^{3-}$ |
| M–O | 176 | 177 |
| M–Cl | 284 | 281 |
| O–M–O | 103 | 102 |
| Cl–M–Cl | 83 | 82 |
| O–M–Cl | 165 | 165 |

The functional and basis-set choices were based on the results of tests performed on several $[\text{MO}_4]$ and $[\text{M}_2\text{O}_7]$ species.^{14,15} Geometry optimizations were carried out using LDA methods, whereas data on thermochemistry and energetics were extracted from single-point BP86 calculations. The highest possible molecular symmetry was utilized, namely, C_{4v} , C_{2v} , and C_{3v} for $[\text{MOCls}]^n$, $[\text{MO}_2\text{Cl}_4]^n$, and $[\text{MO}_3\text{Cl}_3]^n$ complexes, respectively. Bond indexes were obtained according to the definition proposed by Mayer,^{22,23} with a program²⁴ designed for their calculation from the ADF output file. Graphics of molecular orbitals were generated with the MOLEKEL²⁵ program.

Results and discussion

Structural properties

The structural parameters and M–O vibrational frequencies of all complexes investigated are summarized in Tables 1 through 3, and structural schemes showing atom labels are given in Fig. 1. Where possible, comparisons with experimental data (obtained from crystal-structure studies reported in the literature)^{26–35} are included. For V, Nb, and Ta, results are only given for the (formally) d^0 $[\text{MOCls}]^{2-}$ complexes, because convergence difficulties rendered the geometry optimizations of the more negatively charged and reduced species unfeas-

Table 3 M–O stretching frequencies (in cm^{-1}). Available experimental results are given in parentheses

| Complex | Frequencies A ₁ | |
|---|-------------------------------|----------------|
| [VOCl ₃] ²⁻ | 1023 | |
| [NbOCl ₃] ²⁻ | 924 | |
| [TaOCl ₃] ²⁻ | 914 | |
| [MoOCl ₃] ⁻ | 953 | |
| [MoOCl ₃] ²⁻ | 949 (950) | |
| [MoOCl ₃] ³⁻ | 953 | |
| [WOCl ₃] ⁻ | 958 (955) | |
| [WOCl ₃] ²⁻ | 952 (954) | |
| [WOCl ₃] ³⁻ | 948 | |
| | A ₁ | B ₁ |
| [MoO ₂ Cl ₄] ²⁻ | 924 (933) | 905 (898) |
| [MoO ₂ Cl ₄] ³⁻ | 885 | 818 |
| [WO ₂ Cl ₄] ²⁻ | 944 (936) | 911 (889) |
| [WO ₂ Cl ₄] ³⁻ | 898 | 808 |
| | A ₁ | E |
| [MoO ₃ Cl ₃] ³⁻ | 898 | 855 |
| [WO ₃ Cl ₃] ³⁻ | 918 | 856 |

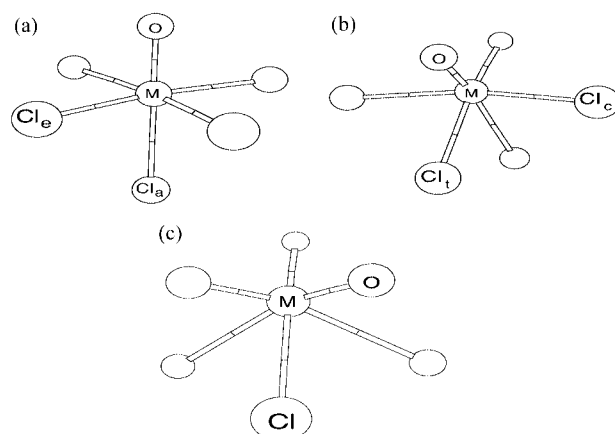


Fig. 1 Structural schemes showing atom labels: (a) $[\text{MOCls}]^n$, (b) $[\text{MO}_2\text{Cl}_4]^n$, (c) $[\text{MO}_3\text{Cl}_3]^n$.

ible or unreliable. Similar difficulties were encountered in the optimizations of Mo and W $[\text{MO}_2\text{Cl}_4]^{4-}$ systems.

An interesting structural feature of complexes containing metal–ligand multiple bonds (also observed in polyoxoanions) is the so-called “*trans* influence”. This has been defined as “the ability of a ligand to lengthen (and apparently weaken) the bond to the ligand *trans* to it”.³⁶ In addition to the lengthening of the bond distance to the *trans* ligand, a bending of the *cis* ligands away from the multiple bond is normally observed. Consequently, six-coordinate units such as those found in simple oxo complexes and polyoxometalates are characterized as a distorted octahedral arrangement, in which the central metal atom has been displaced towards the multiply-bonded ligands.

The *trans* influence is observed in all complexes studied in the present work, the lengthening of the *trans*-chloro bond distances, with respect to those of the corresponding *cis*-chloro ligands, ranging from four to nine percent. The magnitude of this effect is slightly greater in V, Nb, and Ta systems than in the corresponding Mo and W species, and tends to increase as the complexes are reduced. These observations reveal a connection

Table 4 Mulliken charges and metal orbital populations for Mo and W complexes

| Complex | Charges | | | | M orbitals | | |
|---|---------|-------|-----------------|-----------------|------------|------|------|
| | M | O | Cl _c | Cl _a | s | p | d |
| [MoOCl ₅] [−] | 1.15 | −0.51 | −0.31 | −0.39 | 0.21 | 0.50 | 4.15 |
| [MoOCl ₅] ^{2−} | 1.28 | −0.60 | −0.53 | −0.57 | 0.18 | 0.36 | 4.18 |
| [MoOCl ₅] ^{3−} | 1.36 | −0.69 | −0.73 | −0.75 | 0.14 | 0.20 | 4.31 |
| <hr/> | | | | | | | |
| | M | O | Cl _c | Cl _t | s | p | d |
| [MoO ₂ Cl ₄] ^{2−} | 1.52 | −0.62 | −0.54 | −0.60 | 0.17 | 0.33 | 3.98 |
| [MoO ₂ Cl ₄] ^{3−} | 1.54 | −0.73 | −0.74 | −0.80 | 0.15 | 0.23 | 4.07 |
| <hr/> | | | | | | | |
| | M | O | Cl | | s | p | d |
| [MoO ₃ Cl ₃] ^{3−} | 1.73 | −0.76 | −0.82 | | 0.15 | 0.24 | 3.88 |
| <hr/> | | | | | | | |
| | M | O | Cl _c | Cl _a | s | p | d |
| [WOCl ₅] [−] | 1.10 | −0.54 | −0.29 | −0.40 | 0.42 | 0.58 | 3.89 |
| [WOCl ₅] ^{2−} | 1.25 | −0.64 | −0.51 | −0.57 | 0.37 | 0.42 | 3.94 |
| [WOCl ₅] ^{3−} | 1.36 | −0.74 | −0.71 | −0.74 | 0.31 | 0.24 | 4.13 |
| <hr/> | | | | | | | |
| | M | O | Cl _c | Cl _t | s | p | d |
| [WO ₂ Cl ₄] ^{2−} | 1.56 | −0.67 | −0.51 | −0.59 | 0.34 | 0.39 | 3.72 |
| [WO ₂ Cl ₄] ^{3−} | 1.59 | −0.79 | −0.72 | −0.79 | 0.30 | 0.26 | 3.85 |
| <hr/> | | | | | | | |
| | M | O | Cl | | s | p | d |
| [WO ₃ Cl ₃] ^{3−} | 1.84 | −0.81 | −0.80 | | 0.29 | 0.25 | 3.62 |

between the total charge of the molecules and the *trans* influence, and thus appear to support the explanation for this phenomena that focuses on the repulsive interactions between the ligands.³⁶ Nevertheless, examination of the Mo and W (formally) d⁰ series shows that although the *trans*-chloro bonds do lengthen as the systems become increasingly negative, there is also a connection between the bond distances and the number of multiply-bonded ligands in the complex. Therefore, electronic (bonding-related) factors must also be considered, and further discussions are included in the next sections.

Experimental information on this set of chloro-oxo-metalate complexes is scarce, but for those cases where data are available, computational results compare well with the crystal-structure parameters. A poor agreement between calculation and experiment is only found for the W–Cl_a distance in [WOCl₅][−], although in this case the observed bond length is clearly rather longer than expected from comparison with [WOCl₅]^{2−}, possibly as a consequence of the Cl_a atom being involved in a weak interaction with the cation. This has been detected in [NbOCl₅]^{2−}, where one of the Nb–Cl bonds has been lengthened by hydrogen bonding to the Cl ligand.²⁶

In general, the characteristic parameters of the MO_n fragments are largely insensitive to the actual chemical structure of the rest of the molecule, and thus the present results can be compared with those for six-coordinate oxo complexes containing different ligands. Bond lengths and angles predicted by the present calculations are found to fall within or close to the typical experimental ranges³⁶ (V–O: 154–164 pm, Nb–O: 168–177 pm, Ta–O: 173 pm, Mo–O: 162–180 pm, W–O: 157–177 pm; O–M–O: 102–112°), and it is also observed that the calculated bending of *cis* ligands away from the metal–oxo moiety in [MOCl₅] species is in accord with experimental

results, these values ranging from 95° to 104° in a variety of complexes.

The agreement between calculation and experiment extends to the M–O stretching frequencies in Table 3. Available experimental values are closely reproduced, and calculated frequencies for all [MOCl₅]^{*n*−} species compare satisfactorily with results typically observed for mono-oxo complexes³⁶ (V–O: 875–1035 cm^{−1}, Nb–O: 875–1020 cm^{−1}, Ta–O: 905–935 cm^{−1}, Mo–O: 922–1050 cm^{−1}, W–O: 922–1058 cm^{−1}).

Bonding analysis

General considerations. Mulliken charges and metal basis-function populations for the complete series of Mo and W complexes investigated are shown in Table 4. A rather surprising result is the (small) increase in the charge, and corresponding decrease in total orbital population, on the metal centres as the molecules are reduced. The electronic configuration of Mo and W in all species is close to d⁴ (compared to the formal d⁰, d¹, or d² assignments) and remains relatively unperturbed by reduction.

The population of the d-type functions does increase on reduction, in accordance with the changes in the character of the frontier orbitals, which become more M d-like (Table 5), but the p orbitals, and to a lesser extent the s orbitals, are primarily responsible for the (in principle unexpected) general results. In all complexes, although the s-type and p-type functions are sparsely populated and make minor contributions to bonding, the decrease in their populations on reduction is large enough to surpass the increase in the d-orbital populations, and leads to slightly higher charges. The effects on the metal atoms are consistent with the fact that the excess negative charge of the

Table 5 Composition of frontier orbitals in $[\text{MOCl}_5]^{n-}$ and $[\text{MO}_2\text{Cl}_4]^{n-}$ complexes of Mo and W (LU: lowest unoccupied, SO: singly occupied, HO: highest occupied, MO: molecular orbital)

| Orbital $2b_2$ | Complex | Character | |
|-------------------|-------------------------|-----------|------|
| | | M d | Cl p |
| LUMO | $[\text{MoOCl}_5]^-$ | 0.56 | 0.38 |
| SOMO | $[\text{MoOCl}_5]^{2-}$ | 0.67 | 0.32 |
| HOMO | $[\text{MoOCl}_5]^{3-}$ | 0.84 | 0.15 |
| LUMO | $[\text{WOCl}_5]^-$ | 0.61 | 0.36 |
| SOMO | $[\text{WOCl}_5]^{2-}$ | 0.69 | 0.30 |
| HOMO | $[\text{WOCl}_5]^{3-}$ | 0.84 | 0.15 |

| $7b_1$ | Complex | Character | |
|--------|----------------------------------|-----------|------|
| | | M d | O p |
| LUMO | $[\text{MoO}_2\text{Cl}_4]^{2-}$ | 0.58 | 0.24 |
| SOMO | $[\text{MoO}_2\text{Cl}_4]^{3-}$ | 0.65 | 0.22 |
| LUMO | $[\text{WO}_2\text{Cl}_4]^{2-}$ | 0.62 | 0.24 |
| SOMO | $[\text{WO}_2\text{Cl}_4]^{3-}$ | 0.70 | 0.21 |

reduced systems is mainly distributed over the Cl ligands and causes the M–Cl bonds to become more ionic.

Mayer indexes are summarized in Table 6 (M–O) and 7 (M–Cl). A symmetry-based decomposition of the M–O bond orders is also included. Multiple bonding is predicted for all metal–oxo moieties, and for the (formally) d^0 series of Mo and W, the indexes are found to decrease as the number of M–O bonds increases, as expected.³⁶

In spite of the differences in bond multiplicity, all the metal–ligand (M–L) interactions studied are similar in character (Fig. 2), as they involve mostly contributions from M d-type and L (O or Cl) p-type functions. The oxygen and chlorine s orbitals lie low in energy, and are separated from the metal orbitals by a sufficiently large gap to render their bonding interactions unfavourable.

Molecular-orbital description. Schematic representations of the molecular-orbital diagrams of the three classes of complexes studied in this work are given in Fig. 2. These schemes are entirely qualitative (in the sense that no accurate quantitative correlations exist amongst the positions of atomic and molecular energy levels), and are intended to summarize the

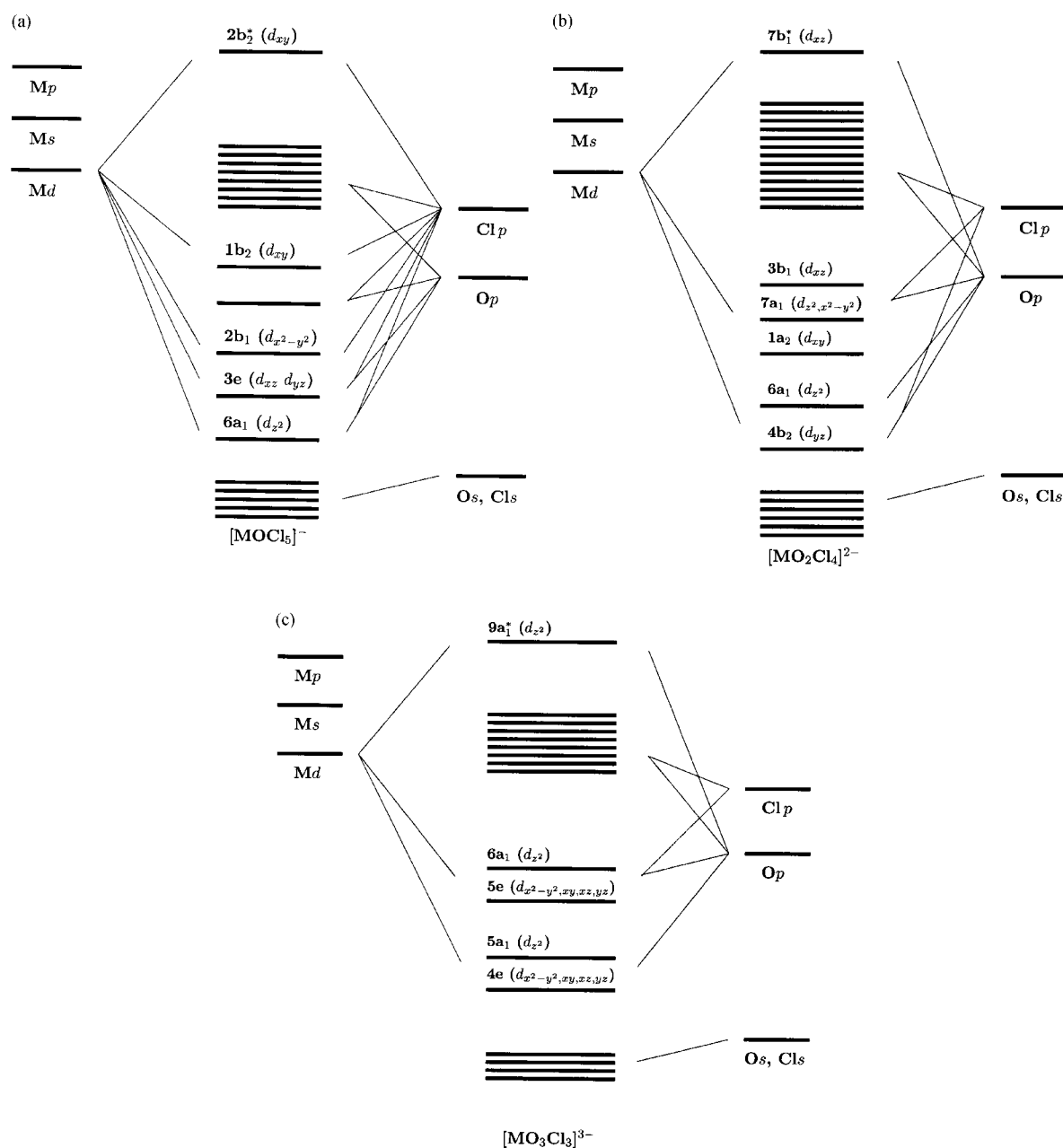


Fig. 2 Qualitative molecular-orbital diagrams showing (predominant) M, O, and Cl contributions: (a) $[\text{MOCl}_5]^-$, (b) $[\text{MO}_2\text{Cl}_4]^{2-}$, (c) $[\text{MO}_3\text{Cl}_3]^{3-}$.

Table 6 Mayer indexes for M–O bonds

| Molecule | Bond order | Decomposition | |
|----------------------------------|------------|---------------|-------------|
| | | a_1 | e |
| $[\text{VOCl}_5]^{2-}$ | 2.04 | 0.58 | 1.46 |
| $[\text{NbOCl}_5]^{2-}$ | 1.87 | 0.57 | 1.30 |
| $[\text{TaOCl}_5]^{2-}$ | 1.87 | 0.61 | 1.26 |
| $[\text{MoOCl}_5]^-$ | 1.83 | 0.53 | 1.30 |
| $[\text{MoOCl}_5]^{2-}$ | 1.86 | 0.56 | 1.30 |
| $[\text{MoOCl}_5]^{3-}$ | 1.91 | 0.61 | 1.30 |
| $[\text{WOCl}_5]^-$ | 1.85 | 0.57 | 1.28 |
| $[\text{WOCl}_5]^{2-}$ | 1.87 | 0.60 | 1.27 |
| $[\text{WOCl}_5]^{3-}$ | 1.89 | 0.64 | 1.25 |
| | | $b_2 + a_1$ | $a_2 + b_1$ |
| $[\text{MoO}_2\text{Cl}_4]^{2-}$ | 1.75 | 1.03 | 0.72 |
| $[\text{MoO}_2\text{Cl}_4]^{3-}$ | 1.68 | 1.12 | 0.55 |
| $[\text{WO}_2\text{Cl}_4]^{2-}$ | 1.76 | 1.06 | 0.70 |
| $[\text{WO}_2\text{Cl}_4]^{3-}$ | 1.65 | 1.14 | 0.51 |
| | | a_1 | e |
| $[\text{MoO}_3\text{Cl}_3]^{3-}$ | 1.62 | 0.33 | 1.29 |
| $[\text{WO}_3\text{Cl}_3]^{3-}$ | 1.62 | 0.37 | 1.25 |

Table 7 Mayer indexes for M–Cl bonds

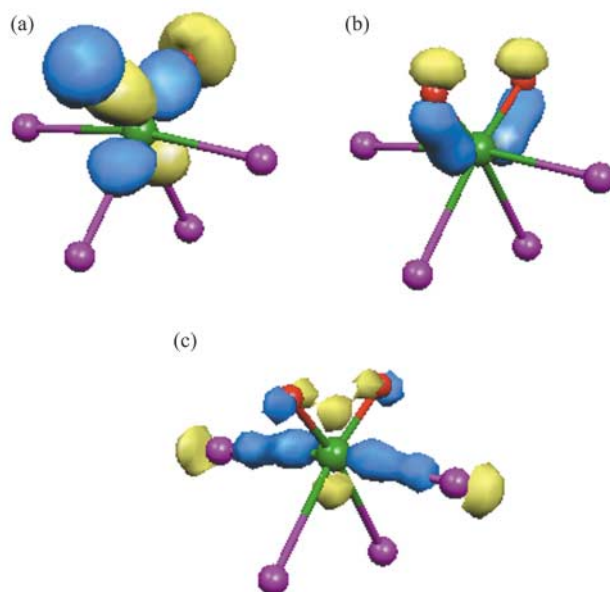
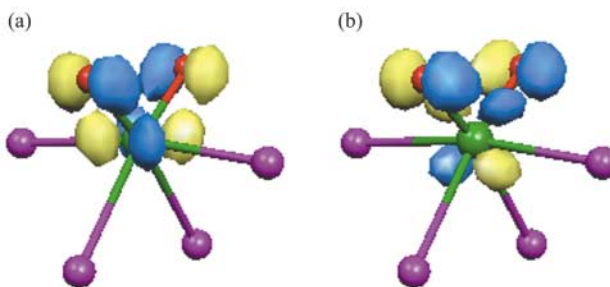
| Molecule | M–Cl _e | M–Cl _a |
|----------------------------------|-------------------|-------------------|
| $[\text{VOCl}_5]^{2-}$ | 0.90 | 0.71 |
| $[\text{NbOCl}_5]^{2-}$ | 0.73 | 0.58 |
| $[\text{TaOCl}_5]^{2-}$ | 0.76 | 0.56 |
| $[\text{MoOCl}_5]^-$ | 0.91 | 0.85 |
| $[\text{MoOCl}_5]^{2-}$ | 0.66 | 0.64 |
| $[\text{MoOCl}_5]^{3-}$ | 0.44 | 0.41 |
| $[\text{WOCl}_5]^-$ | 0.96 | 0.83 |
| $[\text{WOCl}_5]^{2-}$ | 0.68 | 0.63 |
| $[\text{WOCl}_5]^{3-}$ | 0.47 | 0.41 |
| | | |
| | M–Cl _e | M–Cl _i |
| $[\text{MoO}_2\text{Cl}_4]^{2-}$ | 0.65 | 0.59 |
| $[\text{MoO}_2\text{Cl}_4]^{3-}$ | 0.37 | 0.31 |
| $[\text{WO}_2\text{Cl}_4]^{2-}$ | 0.70 | 0.59 |
| $[\text{WO}_2\text{Cl}_4]^{3-}$ | 0.42 | 0.32 |
| | | |
| | M–Cl | |
| $[\text{MoO}_3\text{Cl}_3]^{3-}$ | 0.27 | |
| $[\text{WO}_3\text{Cl}_3]^{3-}$ | 0.31 | |

most general and representative characteristics of the electronic structures of the species investigated, by highlighting the major atomic contributions to the molecular orbitals.

The diagrams shown in Fig. 2 correspond to Mo systems, but those for W systems exhibit only small differences. The levels that are most important for M–L bonding are identified with their symmetry labels. The molecular orientation has been selected so that the C_4 ($[\text{MOCl}_5]^{n-}$), C_2 ($[\text{MO}_2\text{Cl}_4]^{n-}$, the MO_2 unit lies in the yz plane), or C_3 ($[\text{MO}_3\text{Cl}_3]^{n-}$) axis coincides with the z axis.

In (C_{4v}) mono-oxo complexes, the metal d orbitals transform as the a_1 (d_{z^2}), b_1 ($d_{x^2-y^2}$), b_2 (d_{xy}), and e (d_{xz} , d_{yz}) irreducible representations. The d_{z^2} (σ) and d_{xz}/d_{yz} (π) functions are used in interactions with the axial ligands, a triple M–O bond thus being possible. Bonding to equatorial ligands can involve all five M d-orbitals, of which the $d_{x^2-y^2}$ and d_{xy} functions are restricted (by symmetry) to participate in exclusively M–L_e interactions.

In (C_{2v}) *cis* di-oxo species, the symmetry classification of the metal d orbitals is a_1 (d_{z^2} , $d_{x^2-y^2}$), a_2 (d_{xy}), b_1 (d_{xz}), and b_2 (d_{yz}). Five molecular orbitals (two of a_1 symmetry, one each of a_2 , b_1 , and b_2 symmetry) are most significant for M–L bonding. All of these are involved in the MO_2 unit, giving a possible bond order of 2.5 for each M–O fragment. Figs. 3 and 4 show that these five

**Fig. 3** In-plane M–O bonding interactions in $[\text{MO}_2\text{Cl}_4]^{2-}$ complexes: (a) b_2 orbitals, (b) and (c) a_1 orbitals.**Fig. 4** Out-of-plane M–O bonding interactions in $[\text{MO}_2\text{Cl}_4]^{2-}$ complexes: (a) a_2 orbitals, (b) b_1 orbitals.

orbitals can be divided into a $b_2 + a_1$ set representing in-plane bonding, and an $a_2 + b_1$ set describing out-of-plane interactions. The M–Cl_i bonds are primarily described by the $6a_1$ orbital, whereas the M–Cl_e bonds are represented in the higher-lying ($1a_2$, $7a_1$, $3b_1$) set.

In (C_{3v}) tri-oxo systems, the metal d-type functions are divided into a_1 (d_{z^2}) and e ($d_{x^2-y^2}$, d_{xy} , d_{xz} , d_{yz}) species. Six molecular orbitals (two of a_1 and four of e symmetry) participate in the formation of three M–O bonds, each of which could therefore be described (in principle) as a double bond. Bonding to Cl ligands is highly ionic, but there is also some covalent character that can be associated with the $5e$ and $6a_1$ levels.

The maximized bond-order values of 3.0, 2.5, and 2.0 for the M–O interactions in $[\text{MOCl}_5]^{n-}$, $[\text{MO}_2\text{Cl}_4]^{n-}$, and $[\text{MO}_3\text{Cl}_3]^{n-}$ complexes, respectively, are possible if the metal–oxo moieties are treated as separate and fully covalent entities. In the actual

molecules, the metal orbitals involved in M–O interactions are also employed for M–Cl bonding, and ionic contributions are important. This results in a reduction of electron density at the M–O bonds, and is reflected by the smaller values of the calculated bond indexes.

[MOCl₃]^{n−} Complexes. The total M–O bond orders for mono-oxo species can be decomposed into a_1 and e contributions representing, respectively, σ and π bonding. The results in Table 6 correlate with the vibrational data in Table 3, and suggest that the metal–oxo bonds in the V complex may be stronger than those in the heavier-element systems, particularly as a consequence of more favourable Md–Op π -type interactions. The M–Cl indexes are somewhat greater for *cis*-ligand bonds than they are for the *trans*-ligand bond, in accord with the shorter lengths and lower ionicity of the former. Also, the difference between the values for *cis*-ligand and *trans*-ligand bonds shows a correlation with the magnitude of the *trans* influence, both being greater for V, Nb, and Ta than for Mo and W ('Structural properties' section). In particular, the M–Cl bond-order difference and the *trans* influence reach their smallest values in the Mo species. Thus, these results appear supportive of the need to consider electronic factors as well as electrostatic effects.

The structural data for [MOCl₃]^{n−} complexes (Table 1) shows that M–O distances are not affected by reduction, and the Mayer-index values indicate that these bonds may become slightly stronger, in particular the σ interactions, π bonding remaining comparatively unchanged. On the other hand, a considerable lengthening of the M–Cl distances is observed, and this is reflected by a significant decrease in the bond orders, which is also in accordance with the increasingly ionic character of the M–Cl bonds revealed by the Mulliken charges (Table 4).

The present calculations support the general features of the Ballhausen–Gray (BG)^{37,38} model for the electronic structure of C_{4v} oxo complexes, namely, a LUMO with M d_{xy} character in (formally) d⁰ systems and, consequently, a ²B₂ ground state for the one-electron reduced species. For the Mo and W [MOCl₃]^{3−} species, the singlet corresponding to the 2b₂² configuration has been found to be the ground state.

The BG picture provides the basis for the rationalization of type-I polyoxoanion redox behaviour in terms of the bonding properties of [MOL₃] monomers, as described in the 'Introduction' section. However, some of its assumptions—participation of M s and p orbitals, and neglect of M–L π bonding—are not realized in the present results. It has been mentioned that the M–O and M–Cl bonds contain minor contributions from metal s- and p-type functions, and, from Table 5 and Fig. 5, it is clear

that although the LUMO is M–O nonbonding and possesses substantial M d_{xy} character (that increases with reduction), it also represents a π -like antibonding interaction between the metal atom and the equatorial (*cis*) ligands.

The observations in the preceding paragraph are consistent with the invariance of M–O distances and the elongation of M–Cl_e bonds caused by reduction. The latter is probably a combined consequence of the occupation of the M–Cl_e antibonding 2b₂ orbital, and the increasing repulsion brought about by the higher charges on the Cl atoms. These repulsive interactions must also be contributing to pushing the *trans* ligand away from the metal centre, but the (apparently) greater concentration of electron density at the M–O bonds may be equally involved in this effect. The lengthening of M–Cl_a bonds therefore seems to provide evidence for the interplay of electrostatic and electronic factors as a cause for the *trans* influence.³⁶

[MO₂Cl₄]^{n−} Complexes. The M–O bonds in the Mo and W di-oxo complexes are observed to lengthen by 2 pm and their Mayer indexes are predicted to decrease as the species are reduced, in agreement with the metal–oxo antibonding nature of the frontier orbitals. Details about the composition and character of these orbitals are given in Table 5 and Fig. 5. They are π -like combinations of M d_{xz} and O p_x functions with significantly more metal than oxygen character in both oxidized and reduced systems. It is interesting to note that although the overall values diminish with reduction, the in-plane contributions ($b_2 + a_1$) to the M–O bond orders are found to increase.

As in mono-oxo complexes, on reduction, a considerable decrease in the Mayer indexes, and increase in the length and ionicity of the M–Cl bonds are observed. The interactions involving *cis* ligands appear stronger than those between the metal and *trans* Cl atoms, as suggested by the shorter M–Cl_e distances.

An important structural change occurs in the Cl_e–M–Cl_e unit of the reduced complexes. The *cis* ligands bend towards the M–O bonds, instead of away from them (as more frequently observed³⁶). This is probably caused by the increased repulsion between Cl_e and Cl_i centres, and may also be favoured by reduced electron density at the multiply bonded MO₂ fragment. This phenomenon may also explain why the $b_2 + a_1$ M–O index becomes greater. The *cis* ligands are lying out of the plane containing the di-oxo moiety, and their displacement towards the latter seems to be forcing some density from the $a_2 + b_1$ (out-of-plane) bonds into the $b_2 + a_1$ (in-plane) orbitals.

[MO₃Cl₃]^{3−} Complexes. In tri-oxo species, a simple separation of the bonding contributions into σ and π , or in-plane and out-of-plane types is not possible. Nevertheless, it is useful to calculate a_1 (M d_{z²}) and e (M d_{x²−y²}, d_{xy}, d_{xz}, and d_{yz}) indexes, which show that all five metal d-type functions make relatively similar contributions to the M–O orbital interactions. As in [MO₂Cl₄]^{2−} systems, the LUMO of [MO₃Cl₃]^{3−} complexes is of Md–Op and π -antibonding character, but the metal orbital involved is the d_{xy} function (Fig. 5). The M–Cl bonds are appreciably longer, more ionic, and weaker than they are in the mono-oxo and *cis* di-oxo (formally) d⁰ counterparts, apparently reflecting the consequences of a stronger *trans* influence.

Oxidized series. It has been mentioned that across the (formally) d⁰ series—[MOCl₃][−], [MO₂Cl₄]^{2−}, [MO₃Cl₃]^{3−}—it is observed that, as the total molecular charge increases, the Cl atoms become more negative and their corresponding bonds become more ionic and longer. This is reflected by the decrease in the Mayer-index values. This build-up of charge on the Cl centres should lead to stronger repulsions between *cis* and *trans* ligands that would tend to push them away from one another, resulting in longer M–Cl bonds. An apparent connection between the increasing number of M–O bonds and the lengthening of *trans* M–Cl distances has also been pointed out. A

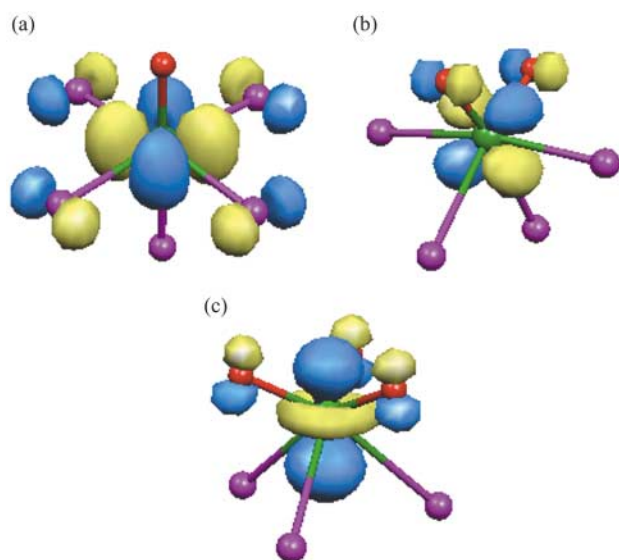


Fig. 5 Frontier orbitals (LUMO) of Mo and W complexes: (a) [MOCl₃]^{3−}, (b) [MO₂Cl₄]^{2−}, (c) [MO₃Cl₃]^{3−}.

Table 8 Fragment analysis (in eV) of *trans* M–Cl bonds

| Molecule | ΔE_B | ΔE_O | ΔE_E |
|----------------------------------|--------------|--------------|--------------|
| $[\text{MoOCl}_5]^-$ | –2.48 | –2.91 | –4.60 |
| $[\text{MoO}_2\text{Cl}_4]^{2-}$ | +1.86 | –1.91 | +0.17 |
| $[\text{MoO}_3\text{Cl}_3]^{3-}$ | +5.77 | –0.94 | +5.21 |
| $[\text{WOCl}_5]^-$ | –2.58 | –3.02 | –5.26 |
| $[\text{WO}_2\text{Cl}_4]^{2-}$ | +1.77 | –2.04 | –0.36 |
| $[\text{WO}_3\text{Cl}_3]^{3-}$ | +5.72 | –1.09 | +4.85 |

greater number of multiply-bonded ligands should translate into a build-up of electron density at the MO_n fragments that could lead to a weakening of the orbital interactions between the metal atom and the *trans* ligands and, therefore, to longer M–Cl bonds. These observations present additional evidence in favour of both electronic and electrostatic reasons being linked with the *trans* influence.

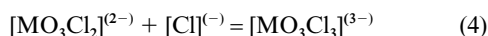
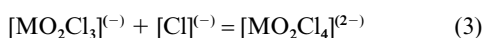
Fragment analysis

The molecular bonding energy (E_B) can be decomposed as:

$$E_B = E_O + E_P + E_E \quad (1)$$

where E_O , E_P , and E_E are, respectively, orbital-mixing, Pauli-repulsion, and electrostatic-interaction terms. Descriptions of the physical significance of these properties have been given by Landrum, Goldberg, and Hoffmann³⁹ and by Baerends and coworkers.¹⁷ Both E_O and E_P represent orbital-interaction effects, but the former is stabilizing whereas the Pauli term is destabilizing. The E_E contribution is primarily dominated by the nucleus–electron attractions, and therefore has a stabilizing influence.

The following fragment approach to the structure of the chloro-oxo complexes,



combined with eqn. (1), can provide a relative measure of the electronic (orbital) and electrostatic effects on metal bonding to the Cl atoms (in *trans*-to-oxo arrangement), across the oxidized (formally d^0) series.

The total molecular bonding energy relative to the fragments is given by:

$$\Delta E_B = \Delta E_O + \Delta E_P + \Delta E_E \quad (5)$$

A summary of the results of calculations based on eqns. (2) through (5) is given in Table 8. The trends observed confirm the conclusions drawn from the structural and Mulliken–Mayer analyses. As the number of oxo ligands increases, the *trans* M–Cl bonds become longer and weaker due to electronic (ΔE_O) and electrostatic (ΔE_E) destabilization.

It has been mentioned in the ‘Introduction’ that the rather different redox behaviour of type-I and type-II polyanions is usually explained in terms of the distinct properties of the LUMOs in the respective model monomeric oxo complexes. A comparison of the changes in bonding and orbital energy in the oxidized and one-electron reduced $[\text{MOC}_l_5]^{(n-)}$ and $[\text{MO}_2\text{Cl}_4]^{(n-)}$ species is given in Table 9. The analysis is based on:

$$\delta E_{B/O} = \frac{E_{B/O}(r) - E_{B/O}(o)}{E_{B/O}(o)} \quad (6)$$

Table 9 Changes (percentage) to the bonding (δE_B) and orbital (δE_O) energy caused by one-electron reduction of $[\text{MOC}_l_5]^{(n-)}$ and $[\text{MO}_2\text{Cl}_4]^{(n-)}$ complexes

| Molecule | (δE_B) | (δE_O) |
|------------------------------------|----------------|----------------|
| $[\text{MoOCl}_5]^{(n-)}$ | –0.6 | –6.2 |
| $[\text{MoO}_2\text{Cl}_4]^{(n-)}$ | –15.1 | –16.1 |
| $[\text{WOCl}_5]^{(n-)}$ | –2.3 | –7.7 |
| $[\text{WO}_2\text{Cl}_4]^{(n-)}$ | –16.7 | –17.2 |

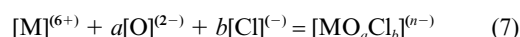
Table 10 Changes (percentage) to the bonding (ΔE_B) and orbital-mixing (ΔE_O) energy caused by removal of metal s and p valence functions

| Molecule | $\delta(\Delta E_B)$ | $\delta(\Delta E_O)$ |
|----------------------------------|----------------------|----------------------|
| $[\text{MoOCl}_5]^-$ | –1.1 | –3.2 |
| $[\text{MoO}_2\text{Cl}_4]^{2-}$ | –0.8 | –2.8 |
| $[\text{MoO}_3\text{Cl}_3]^{3-}$ | –0.7 | –2.5 |
| $[\text{WOCl}_5]^-$ | –1.2 | –3.9 |
| $[\text{WO}_2\text{Cl}_4]^{2-}$ | –0.8 | –2.8 |
| $[\text{WO}_3\text{Cl}_3]^{3-}$ | –0.6 | –2.4 |

where $E(o)$ and $E(r)$ are, respectively, the values of the energy terms for the oxidized and reduced complexes.

The results in Table 9 indicate that there is a considerably stronger reduction-driven destabilization of *cis* di-oxo than mono-oxo species, and the orbital-interaction contribution is also significantly more unfavourably affected in the former than the latter. However, it is important to note that the orbital-mixing energy for both types of model complexes is smaller in the reduced systems, as the corresponding LUMOs are antibonding. The greater magnitude of the destabilization in $[\text{MO}_2\text{Cl}_4]^{(n-)}$ with respect to $[\text{MOC}_l_5]^{(n-)}$ lies in that these orbitals are M–O antibonding in the former but M–O nonbonding in the latter (although they are globally antibonding due to the effect of M–Cl_c interactions). These observations are in satisfactory agreement with experimental data indicating that type-I polyanions are more easily reduced than type-II polyanions.

The molecular-orbital and population analyses suggest that the bonding contributions from metal s and p functions are minor, as pointed out in preceding sections. This phenomenon can also be explored by means of a fragment-decomposition approach. The structures of the complexes are described as:



and calculations are carried out both with and without metal s and p valence orbitals. The relative effect of removing these orbitals can be measured as:

$$\delta(\Delta E_{B/O}) = \frac{\Delta E_{B/O}(d) - \Delta E_{B/O}(dsp)}{\Delta E_{B/O}(dsp)} \quad (8)$$

The results from the application of eqns. (7) and (8) to the oxidized series of Mo and W complexes are summarized in Table 10, and support the general description of the M–L bonds as predominantly Md–Lp in character. The contributions from metal s and p orbitals are approximately one percent if the total bonding energy is considered, and between two and four percent in the case of the orbital-interaction term. The data in Table 10 also correlate satisfactorily with the fact that M s and p functions are “more involved” in M–Cl than M–O bonding, as shown by the reduction of the $\delta(\Delta E_{B/O})$ values with decreasing numbers of Cl atoms.

Conclusion

The molecular structures and metal–oxo vibrational frequencies of a set of chloro-oxo-metalate complexes have been calculated using density-functional theory. The computed geometrical and vibrational parameters compare well with available experimental information. *Trans*-influence phenomena affecting the Cl ligands have been observed in all species, and on the basis of structural, Mulliken–Mayer, and bonding-energy analyses it has been concluded that the most likely cause is an interplay of electrostatic and electronic factors, as suggested in the literature.

The properties of the frontier orbitals of mono-oxo and *cis* di-oxo complexes, obtained from the present high-level calculations, fit into the general features of the simpler molecular-orbital descriptions usually employed in modelling electron-transfer behaviour of type-I and type-II polyoxo-metalates, but there are also some important particular discrepancies. For example, although the LUMO of the $[\text{MOC}_3]^{n-}$ species is M–O nonbonding as described in the literature its M–Cl₂ antibonding character is significant but has been frequently ignored.

The general conclusions concerning the electronic structure of the oxo systems investigated are similar to those drawn by Frenking and coworkers from their study of a series of nitrido and oxo complexes of Mo, W, Re, and Os,¹¹ and can be summarized by the following remarks: metal–ligand bonds possess Md–Lp character, metal–oxo interactions are strongly covalent but metal–chloro interactions, especially in reduced species, exhibit considerable ionic character, and Mulliken charges and d-orbital populations for the metal atoms are significantly lower and higher, respectively, than the formal oxidation states and electronic configurations are.

Acknowledgements

The authors would like to thank EPSRC, the Cambridge Overseas Trust, Selwyn College (Cambridge), and the University of Hull for financial support, and the Computational Chemistry Working Party for access to computational facilities in the Rutherford Appleton Laboratory.

References

- 1 M. T. Pope, *Heteropoly and Isopoly Oxometalates*, Springer-Verlag, Heidelberg, 1983.
- 2 M. T. Pope and A. Müller, *Angew. Chem., Int. Ed. Engl.*, 1991, **30**, 34.
- 3 L. C. W. Baker and D. C. Glick, *Chem. Rev.*, 1998, **98**, 3.
- 4 M. T. Pope and A. Müller, eds., *Polyoxometalates: from Platonic Solids to Anti-retroviral Activity*, Kluwer, Dordrecht, 1994.
- 5 K. Nomiya and M. Miwa, *Polyhedron*, 1984, **3**, 341.
- 6 R. B. King, *Inorg. Chem.*, 1991, **30**, 4437.
- 7 T. R. Cundari, *Chem. Rev.*, 2000, **100**, 807.
- 8 T. R. Cundari and P. D. Raby, *J. Phys. Chem. A*, 1997, **101**, 5783.
- 9 F. A. Cotton and X. Feng, *Inorg. Chem.*, 1996, **35**, 4921.
- 10 M. T. Benson, T. R. Cundari, S. J. Lim, H. D. Nguyen and K. Pierce-Beaver, *J. Am. Chem. Soc.*, 1994, **116**, 3955.
- 11 A. Neuhaus, A. Veldkamp and G. Frenking, *Inorg. Chem.*, 1994, **33**, 5278.
- 12 N. Kaltsoyannis, *J. Chem. Soc., Dalton Trans.*, 1994, 1391.
- 13 R. J. Deeth, *J. Chem. Soc., Dalton Trans.*, 1991, 1895.
- 14 A. J. Bridgeman and G. Cavigliasso, *Polyhedron*, 2001, **20**, 2269.
- 15 A. J. Bridgeman and G. Cavigliasso, *J. Phys. Chem. A*, 2001, **105**, 7111.
- 16 ADF2000.02: E. J. Baerends, D. E. Ellis and P. Ros, *Chem. Phys.*, 1973, **2**, 41; L. Versluis and T. Ziegler, *J. Chem. Phys.*, 1988, **322**, 88; G. te Velde and E. J. Baerends, *J. Comput. Phys.*, 1992, **99**, 84; G. Fonseca Guerra, J. G. Snijders, G. te Velde and E. J. Baerends, *Theor. Chem. Acc.*, 1998, **99**, 391.
- 17 G. te Velde, F. M. Bickelhaupt, E. J. Baerends, C. Fonseca Guerra, S. J. A. van Gisbergen, J. G. Snijders and T. Ziegler, *J. Comput. Chem.*, 2001, **22**, 931.
- 18 S. H. Vosko, L. Wilk and M. Nusair, *Can. J. Phys.*, 1980, **58**, 1200.
- 19 W. Kohn and L. J. Sham, *Phys. Rev. A*, 1965, **140**, 1133.
- 20 A. D. Becke, *Phys. Rev. A*, 1988, **38**, 3098.
- 21 J. P. Perdew, *Phys. Rev. B*, 1986, **33**, 8822.
- 22 I. Mayer, *Chem. Phys. Lett.*, 1983, **97**, 270.
- 23 I. Mayer, *Int. J. Quantum Chem.*, 1984, **26**, 151.
- 24 MAYER. A program to calculate Mayer bond-order indexes from the output of the electronic structure packages GAMESS-UK, GAUSSIAN, and ADF, A. J. Bridgeman, University of Hull, 2001, available from the author on request.
- 25 MOLEKEL. An Interactive Molecular Graphics Tool, S. Portmann and H. P. Lüthi, *Chimia*, 2000, **54**, 766.
- 26 V. U. Müller and I. Lorenz, *Z. Anorg. Allg. Chem.*, 1980, **463**, 110.
- 27 J. Poitras and A. L. Beauchamp, *Can. J. Chem.*, 1994, **72**, 1675.
- 28 P. C. Junk and J. L. Atwood, *J. Chem. Soc., Chem. Commun.*, 1995, 1551.
- 29 P. Schreiber, K. Wieghardt, U. Flörke and H.-J. Haupt, *Z. Naturforsch., Teil B*, 1987, **42**, 1391.
- 30 D. Fenske, K. Stahl, E. Hay and K. Dehnicke, *Z. Naturforsch., Teil B*, 1984, **37**, 850.
- 31 D. Brown, *J. Chem. Soc.*, 1964, 4944.
- 32 W. P. Griffith and T. D. Wickins, *J. Chem. Soc. A*, 1968, 400.
- 33 W. P. Griffith, *J. Chem. Soc. A*, 1969, 211.
- 34 M. G. B. Drew, G. W. A. Fowles, E. M. Page and D. A. Rice, *J. Chem. Soc., Dalton Trans.*, 1981, 2409.
- 35 J. M. Coddington and M. J. Taylor, *J. Chem. Soc., Dalton Trans.*, 1990, 41.
- 36 W. A. Nugent and J. M. Mayer, *Metal–Ligand Multiple Bonds*, Wiley, New York, 1988.
- 37 C. J. Ballhausen and H. B. Gray, *Inorg. Chem.*, 1962, **1**, 111.
- 38 H. B. Gray and C. R. Hare, *Inorg. Chem.*, 1962, **1**, 363.
- 39 G. A. Landrum, N. Goldberg and R. Hoffmann, *J. Chem. Soc., Dalton Trans.*, 1997, 3605.